



HAL
open science

Target-in-the-loop coherent combining of 7 fiber lasers: first results

Pierre Bourdon, Hermance Jacqmin, Laurent Lombard, Béatrice Augere,
Anne Durécu, Didier Goular, Roland Domel, Didier Fleury, Christophe
Planchat, Bastien Rouzé, et al.

► To cite this version:

Pierre Bourdon, Hermance Jacqmin, Laurent Lombard, Béatrice Augere, Anne Durécu, et al.. Target-in-the-loop coherent combining of 7 fiber lasers: first results. OPTRO 2020, Jan 2020, PARIS, France. hal-02486706

HAL Id: hal-02486706

<https://hal.science/hal-02486706v1>

Submitted on 21 Feb 2020

HAL is a multi-disciplinary open access archive for the deposit and dissemination of scientific research documents, whether they are published or not. The documents may come from teaching and research institutions in France or abroad, or from public or private research centers.

L'archive ouverte pluridisciplinaire **HAL**, est destinée au dépôt et à la diffusion de documents scientifiques de niveau recherche, publiés ou non, émanant des établissements d'enseignement et de recherche français ou étrangers, des laboratoires publics ou privés.

TARGET-IN-THE-LOOP COHERENT COMBINING OF 7 FIBER LASERS: FIRST RESULTS

P. Bourdon⁽¹⁾, H. Jacqmin⁽¹⁾, L. Lombard⁽¹⁾, B. Augère⁽¹⁾, A. Durécu⁽¹⁾, D. Goular⁽¹⁾, R. Domel⁽¹⁾,
D. Fleury⁽¹⁾, C. Planchat⁽¹⁾, B. Rouzé⁽¹⁾, T. Huet⁽¹⁾, B. Tanguy⁽¹⁾, B.S. Tan⁽²⁾, J.W. Lam⁽²⁾, K. Lim⁽²⁾

⁽¹⁾ ONERA – The French Aerospace Lab, DOTA, BP 80100, F-91123 Palaiseau, France,
Email: pierre.bourdon@onera.fr

⁽²⁾ DSO National Laboratories, 14 Science Park Drive, Singapore 118226, Singapore

KEYWORDS: Fiber laser, coherent combining, phase control, target-in-the-loop, turbulence mitigation

ABSTRACT:

We developed a laser testbed coherently combining seven 1.5- μm fiber lasers through active phase control, using frequency-tagging to assess the phase fluctuations to be compensated for.

In this paper, we present the testbed and its components as well as the results obtained in direct coherent combining, operated at the output of the lasers, without target-in-the-loop feedback. We then introduce the basic principle and show the first indoor results of target-in-the-loop coherent beam combining experiments at a shorter distance of 15 meters.

We then describe the outdoor facility that was chosen for longer range experiments and show qualitative results and qualitative comparisons of the target-in-the-loop coherent beam combining challenge when the target is moved farther away, increasing the range from 15 meters to up to 1 km.

1. INTRODUCTION

Coherent combining techniques involving active phase control of the laser emitters have demonstrated their potential to power scale continuous-wave fiber lasers through coherent addition of the power emitted by multiple separate amplifiers up to the multi-kilowatt level [1]. Live phase-control using fast electro-optic phase modulators is very effective to achieve low residual phase error and high efficiency coherent beam combining (CBC).

CBC has been demonstrated for a large number of lasers [2] but many realisations use the fact that the laser beams are spatially separated at the output of the lasers, before overlapping after propagation and becoming undistinguishable. While the laser beams are still spatially distinct, it's feasible to measure the phase of each laser and to control this phase in real time to achieve phase-locking.

However, for some applications, such process cannot be applied as phase measurement has to

be done once the laser beams have already begun to overlap and to interfere. That's the case of target-in-the-loop CBC where one wants to phase-lock the lasers on a remote target, maximizing the power density deposited at long range.

In this case, phase measurement at the output of the lasers is useless, as beam propagation induces additional phase shifts that are not accounted for in this measurement. It's necessary to find some way of driving the laser phases, benefiting from the information available in the optical signal backscattered by the remote target.

One approach is to try and maximize the intensity of this backscattered signal, as maximum power density deposited on the target corresponds to a maximum of this backscattered signal too.

It's been done, for instance, very early on, during the first experiments of TIL-CBC on a glint target [3], and, later on, up to 7 km using a stochastic parallel gradient descent algorithm [4], a classical approach to maximize optical intensity by step-by-step optical wavefront correction.

In 2009, our team demonstrated a more practical and promising approach that can be performed using frequency-tagging for CBC phase control [5]. Frequency-tagging each optical channel at a specific frequency to assess the phase fluctuations to be compensated for is an efficient technique for CBC, also known as LOCSET [6]. Frequency-tagging has the advantage of "engraving" specific information on the signal emitted by each optical channel through low-depth modulation. This tagging process enables to easily retrieve the phase information from each channel, within the complex interference signal generated once the laser beams have overlapped. Moreover, this phase information retrieval can also be achieved using the backscattered signal from a remote target.

We also demonstrated that a simple evolution of the configuration of detection used for direct CBC could transform a standard CBC system into a fully operational TIL-CBC device [5].

The tests we performed in 2009 were in the laboratory with artificially generated atmospheric turbulence. In this paper, we present the work done recently to build a testbed coherently

combining seven 1.5- μm fiber lasers through active phase control, using frequency-tagging. We also present the first results obtained on TIL-CBC operating this testbed. These results are obtained propagating the laser beams through the atmosphere, hence through real atmospheric turbulence.

In a first part of this paper, we present the laser testbed and its operation in direct coherent combining, operated at the output of the lasers, without the target in the loop feedback.

In a second part, we present the first results obtained on TIL-CBC when propagating through real turbulence and increasing the propagation range from 15 meters to 1 kilometer.

2. THE LASER TESTBED FOR CBC AND TIL-CBC

The laser configuration is a standard 7-channel master oscillator power amplifier (MOPA) configuration at 1.5 μm wavelength.

A single-frequency low power (40 mW) master oscillator (MO) is split and amplified into 7 channels. Each of the 7 Er-Yb doped fiber amplifiers delivers up to 3 W at 1543 nm.

One of the fiber amplifiers is not phase controlled and is free to fluctuate in phase while in-between the MO and 6 of the amplifiers, we use a fast electro-optic phase modulator with a 150-MHz bandwidth to control the phase of each channel and simultaneously tag each of these 6 channels at a specific frequency around 20 MHz with a low-depth phase modulation.

In this self-referenced LOCSET configuration, the 6 phase-controlled channels follow the phase fluctuations of the seventh channel that's not modulated (see figure 1).

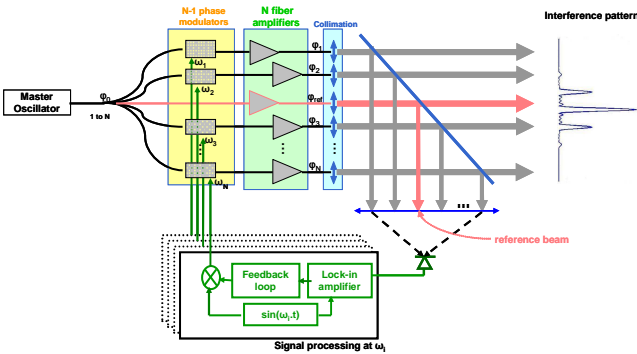


Figure 1. Schematics of the experimental setup for frequency-tagging CBC (also known as LOCSET).

The 7-channel CBC setup delivers a nice interference pattern in the far-field. We confirmed that in direct CBC, i.e. using a fast photodiode to capture part of the central lobe of interference in the far-field, it was easy to lock the phases of the 7 laser channels and stabilize the position of the interference pattern.

In LOCSET, frequency tagging of the i^{th} channel at a specific frequency ν_i results in an interference signal that generates an error signal after

demodulation at the same frequency given by equation (1):

$$i_{error,i}(t) \propto E_i J_1(\beta_i) \left[E_u \sin(\phi_u - \phi_i) + \sum_{j=1}^{N-1} E_j J_0(\beta_j) \sin(\phi_j - \phi_i) \right] \quad (1)$$

where ϕ_i is the i^{th} amplifier chain output phase in the photodetector plane, and ϕ_u the unmodulated reference beam phase in the photodetector plane. E_i and E_u are the respective electric field amplitudes at the output of the i^{th} amplifier and of the unmodulated amplifier. β_i and β_u are the respective modulation depths of the i^{th} amplifier channel and of the unmodulated channel.

Driving the 6 error signals simultaneously to zero in real time results in maintaining equal phases for the 7 channels. Any sudden phase shift is immediately compensated for, thanks to the very fast electro-optic phase modulators and fast detection.

CBC efficiency measured as the fraction of the total power located in the central lobe of the interference pattern was higher than 53 % (see figure 2). It's very close to the experimental maximum that can be achieved with Gaussian laser beams (theoretical maximum is 63 %) taking into account the opto-mechanical constraints limiting the effective fill-factor in the near-field.

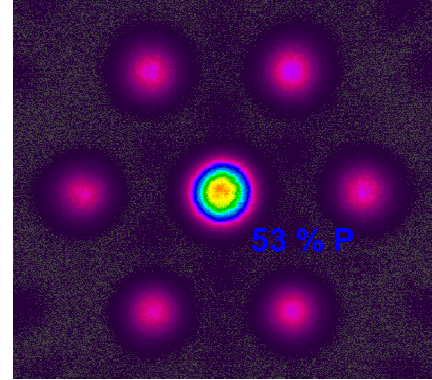


Figure 2. Interference pattern in the far-field, captured on a 1.5- μm camera located at the same distance as the direct CBC detector.

Residual phase error has been measured and is lower than $\lambda/40$, confirming again the high efficiency of the CBC process and the high speed of the feedback loop.

The opto-mechanical head where the outputs of the 7 fiber amplifiers are collimated and sent through the atmosphere is completely adjustable (see figure 3).

Piezo-electric motors are used to set the transverse position of the output fiber tip with respect to the collimating lens, in order to align the 7 collimated beams in the same direction. The focus of the collimating lenses is manually tuned beforehand.

Figure 3 presents pictures of the first part of the testbed dedicated to laser emission.

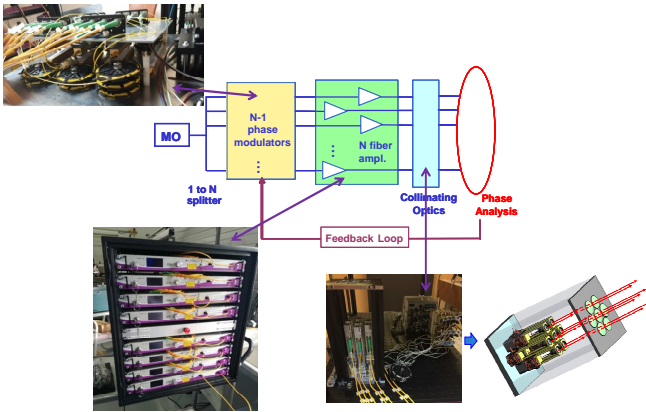


Figure 3. Pictures of the experimental setup parts.

For TIL-CBC, a second stage of the testbed is dedicated to long range focusing of the laser beams and to collection and detection of the backscattered signal from the remote target. We chose to use a bi-static configuration (see figure 4) where the long range focusing and the reception apertures are separated, to limit the risk of narcissus effect, and decrease the optical complexity of the detection line with respects to a monostatic configuration.

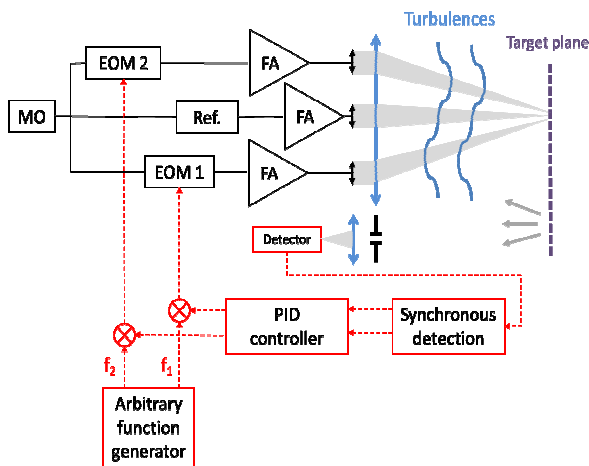


Figure 4. Schematics of the TIL-CBC bi-static configuration. Instead of collecting a fraction of the interference signal between the laser beams at the output of the laser system as in figure 1, the detection line now receives the signal backscattered by the remote target.

3. EXPERIMENTAL DEMONSTRATIONS OF TIL-CBC AT SHORT RANGE

The first experimental tests of TIL-CBC were conducted in the laboratory. As the experiments took place inside closed doors, atmospheric turbulence was very weak and it was easy to achieve similar results in TIL-CBC as in direct CBC.

The target we used was a small diameter high reflectance area obtained by sticking high reflectance tape on a plate and setting up a blackened (i.e. low albedo) aperture in front of this high reflectance target to limit its size.

Indoor one-way TIL-CBC experiments could be conducted up to 15 meters.

We used a large aluminium mirror to fold the optical path back and operate round-trip TIL-CBC experiments in the laboratory up to 30 meters (see figure 5).



Figure 5. Schematics of the experimental setup for 30-m range TIL-CBC with optical path folding mirror to double the range of the experiment. The interference pattern is monitored with a camera located at the same distance from the laser as the target.

In both cases, TIL-CBC operated extremely well, which is not surprising as turbulence was extremely weak.

Next step was to move the testbed to another laboratory to be able to shoot the laser beam outside, propagating through real outdoor turbulence.

Once again, the results were excellent and TIL-CBC operated well. Due to beam wander induced by the outdoor turbulence, TIL-CBC was a little less stable, but we never observed TIL-CBC collapse due to turbulence.

These short range one-way outdoor experiments were conducted up to 45 meters. Using the same metallic mirror as indoors to fold back the optical path, we doubled this range up to 90 meters and still observed very efficient TIL-CBC at this distance (see figure 6).

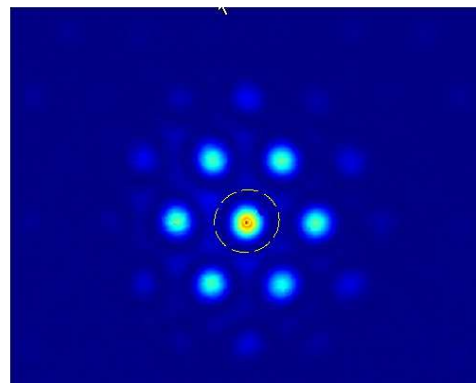


Figure 6. TIL-CBC Interference pattern in the far-field at 90 m, captured on a 1.5- μ m camera located at the same distance as the TIL-CBC target.

We were also able to perform beam-steering, as TIL-CBC was locked on the small diameter target: when moving the target to the right or to the left, the interference pattern will follow the movement of the target. That's just a standard capability of direct frequency-tagging CBC that can be extended to TIL-CBC this way: in direct CBC, when the detector is moved, the interference pattern moves

to follow in order to maximize the power density deposited on the detector.

4. EXPERIMENTAL DEMONSTRATIONS OF TIL-CBC AT LONG RANGE

The testbed has been designed to be mobile and we transferred it to an Onera laser site where we are able to shoot lasers safely up to 1-km range (see figure 7).

The site is equipped with equipment to monitor the weather and atmospheric conditions, and also to measure turbulence strength through the average value of the C_n^2 over 1 km.

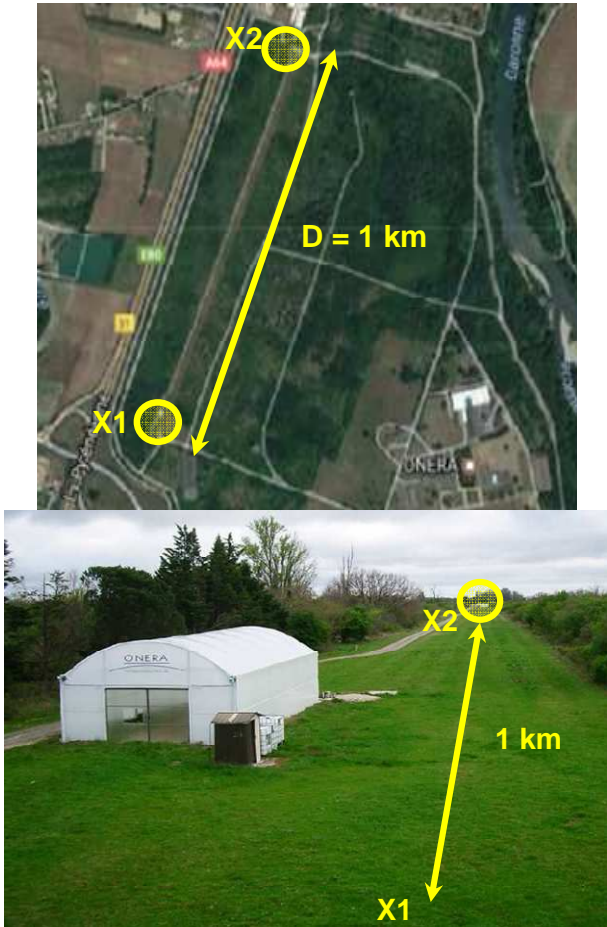


Figure 7. Pictures of the laser site where the long-range TIL-CBC experiments took place.

The experiments took place during summer in the south west of France. As the laser beams propagated horizontally at 1.5 m from the ground, the level of turbulence was quite high and the average value of C_n^2 over 1 km was often close or even much higher than $10^{-13} \text{ m}^{-2/3}$.

Despite these detrimental turbulence conditions, when the C_n^2 value was lower than $10^{-13} \text{ m}^{-2/3}$, we were able to perform efficient TIL-CBC up to 1 km. A transparent wedge plate was placed before the target, to reflect a small fraction of the combined beams power to a black screen located at the same distance as the target.

Proceeding like this, we could record video sequences of the interference pattern displayed on

black screen and observed with an InGaAs Raptor camera, without interfering with the TIL-CBC process in the target plane.

Figure 8 presents instantaneous images of the interference pattern with and without closing the CBC feedback loop.

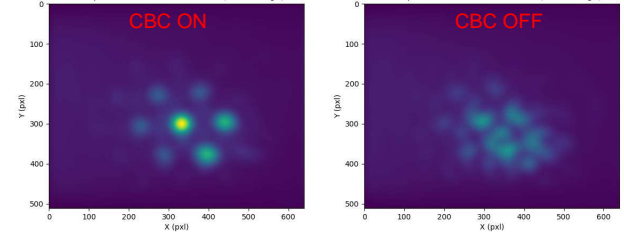


Figure 8. Instantaneous images of the interference pattern generated at 310 m when TIL-CBC feedback loop is active and inactive.

Figure 9 presents averaged images from the same video sequence. The size of the interference lobes is not different in the instantaneous images and in the averaged image, demonstrating that the interference pattern was locked on a fixed position in the target plane.

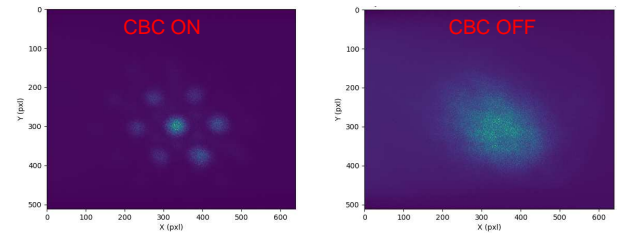


Figure 9. Averaged images of the interference pattern generated at 310 m when TIL-CBC feedback loop is active and inactive.

Figure 10 presents the averaged image obtained when target distance was 1 km.

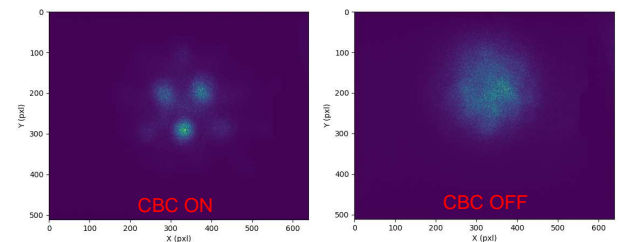


Figure 10. Averaged images of the interference pattern generated at 1 km when TIL-CBC feedback loop is active and inactive.

Even if turbulence induced perturbations clearly appear to decrease the efficiency of the CBC locking process, TIL-CBC still operates and results in an increased power density deposited on the remote target at 1 km.

5. CONCLUSION AND FUTURE WORK

In this paper, we present a mobile testbed for coherent beam combining of 7 fiber lasers emitting at $1.5 \mu\text{m}$. This testbed operates through frequency-tagging phase difference monitoring. It

can concentrate more than 53 % of the overall power in the central of the interference pattern generated in the far-field, after overlap of the laser beams.

The testbed has been designed to use the backscattered signal coming from a remote target as a reference for phase difference monitoring and phase locking. It was operated in a target-in-the-loop configuration, first at short distance in the laboratory, and then at longer distance outdoors, propagating the beams through real, weak to strong atmospheric turbulence.

The longer range outdoor experimental campaign demonstrated that TIL-CBC efficiency is preserved up to more than 310 m. Perturbations induced by strong atmospheric turbulence are significantly affecting TIL-CBC, but TIL-CBC operates at 1 km anyway, however with lower efficiency.

Future work is dedicated to processing the data recorded during this experimental campaign to derive more quantitative results.

6. ACKNOWLEDGEMENTS

This work was funded by DSO National Laboratories, Singapore.

7. REFERENCES

1. Flores, A. Shay, T.M. Lu, C.A. Robin, C. Pulford, B. Sanchez, A.D. Hult D.W. & Rowland K.B. (2011). Coherent beam combining of fiber amplifiers in a kW regime. *Conference CLEO 2011, Paper CFE3*.
2. Bourderionnet, J. Bellanger, C. Primot, J. & Brignon, A. (2011). Collective coherent phase combining of 64 fibers. *Opt. Express* **19**(18), 17053–17058.
3. Pearson, J.E. Bridges, W.B. Hansen, S. Nussmeier, T.A. & Pedinoff M.E (1976). Coherent optical adaptive techniques: design and performance of an 18-element visible multidither COAT system. *Appl. Opt.* **15**(3), 611–621.
4. Weyrauch, T. Vorontsov, M.A. Carhart, G.W. Beresnev, L.A. Rostov, A.P. Polnau, E.E. & Jiang Liu, J. (2011). Experimental demonstration of coherent beam combining over a 7 km propagation path. *Opt. Lett.* **36**(22), 4455–4457.
5. Jolivet, V. Bourdon, P. Bennai, B. Lombard, L. Goular, D. Pourtal, E. Canat, G. Jaouen, Y. Moreau B. & Vasseur O. (2009). Beam shaping of single-mode and multimode fiber amplifier arrays for propagation through atmospheric turbulence, *IEEE J. Sel. Top. Quant. Elec.* **15**(2), 257–268.
6. Shay, T.M. Benham, V. Baker, J.T. Ward, B. Sanchez, A.D. Culpepper, M.A. Pilkington, D. Spring, J. Nelson D.J. & Lu C.A. (2006). First experimental demonstration of self-synchronous phase locking of an optical array, *Opt. Express* **14**(25), 12015–12021.